DOI: https://doi.org/10.68732/6ff3666c0fd67809

ISBN: 978-9989-2053-7-8

Laboratory-Scale Assessment of 2D and 3D Bonded-Particle Models

E. Zengin, Ö. Ündül, Ö. Dinç Göğüş & M. M. Doğu
Istanbul Technical University, Istanbul, Türkiye
eneszengin@itu.edu.tr
0000-0002-5740-7763

Abstract

Discrete Element Method (DEM)-based bonded-particle models are widely used to simulate the mechanical behavior and failure of rock materials. However, the influence of model dimensionality on the representation of deformation, crack development, and failure localization remains an important issue. This study presents a systematic comparison of two-dimensional (2D) and three-dimensional (3D) bonded-particle models calibrated against the same laboratory-derived macroscopic target properties using a consistent calibration flow. Laboratory data obtained from uniaxial compression and indirect tensile strength tests on siltstone samples were used as calibration targets. Both 2D and 3D models were developed in the Particle Flow Code (PFC 7.0) environment using a consistent calibration that matched macroscopic properties, including peak strength, elastic modulus, and stress–strain response. The calibrated models were then evaluated for tensile behavior, crack initiation, and failure patterns. The results show that both models successfully reproduce the overall stress–strain response and peak strength with good agreement. However, significant differences are observed in tensile strength and damage initiation. Both models overestimate tensile strength and predict delayed crack initiation relative to laboratory results, reflecting the known limitations of the classical parallel-bond formulation. In terms of failure behavior, the 2D model exhibits a well-defined, strongly localized failure band, whereas the 3D model shows a more diffuse damage pattern. Analysis of crack distribution and contact-force magnitude indicates that fracture development is dominated by tensile bond breakages and controlled by force-chain reorganization in both models. The findings demonstrate that while 2D bonded-particle models are effective in capturing global mechanical behavior, 3D models provide a more realistic representation of spatially distributed fracture processes. This highlights the importance of model dimensionality in DEM-based simulations and underscores the need to carefully interpret 2D results in the context of real 3D rock behavior.

Keywords

Bonded-particle model, Crack initiation, Dimensionality, Particle Flow Code, Rock mechanics.

1 Introduction

Rock materials play a fundamental role in a wide range of engineering applications, including underground excavations, tunneling, slope stability, and energy-related infrastructure. The mechanical response of these materials under loading conditions governs the safety, performance, and long-term stability of such structures. However, because of their inherently heterogeneous and discontinuous structure—featuring microstructural elements such as grains, pores, and pre-existing flaws—accurately modeling their deformation and failure behavior remains a significant challenge in rock engineering (Potyondy, 2015; Potyondy & Cundall, 2004; Zengin, 2022). Rock engineering problems depend on material strength and are controlled by loading conditions, material heterogeneity, crack development, and progressive failure. As underground openings, slopes, and other rock-supported systems become more complex, understanding how rock deforms and fails under stress becomes increasingly important for both design reliability and hazard assessment (Jing, 2003).

Numerical methods have become important as they provide a means to investigate failure processes that can't be fully captured through laboratory testing or simplified analytical approaches alone (Lisjak & Grasselli, 2014). Among these approaches, discrete and grain-scale methods are particularly valuable for representing fracture initiation, propagation, and interaction in heterogeneous rock materials (Cundall & Strack, 1979; Kong et al., 2024). DEM-based bonded-particle models are particularly suitable for rock mechanics problems because they represent the material as an assembly of interacting particles rather than as a continuous medium. Deformation and failure develop through contact interaction and bond breakage, allowing crack initiation, propagation, coalescence, and localization to emerge directly from the model response (Potyondy & Cundall, 2004). This capability is especially valuable for heterogeneous rock materials, where failure is controlled not only by bulk strength but also by the way microscopic bonds transmit forces, resist deformation, and progressively fail.

Despite their advantages, DEM-based bonded-particle models face a fundamental challenge in establishing a consistent relationship between micro-scale parameters and macro-scale mechanical behavior (Qu et al., 2020; Vallejos et al., 2017). In these models, properties such as stiffness, bond strength, and friction are defined at the particle-contact level, yet the resulting macroscopic response-such as elastic modulus, peak strength, and post-peak behavior-emerges from the collective interaction of thousands of particles. This indirect, highly coupled relationship makes calibration complex and iterative, often needing trial-and-error to match laboratory behavior. Different micro-mechanical parameters can yield similar overall responses, leading to non-uniqueness in calibration and limiting interpretability. A calibrated model might match stress-strain curves but represent different internal damage processes. Therefore, accurately capturing both global responses (stiffness, strength) and local behaviors (crack initiation, propagation, failure mode) remains a key challenge in bonded-particle rock modeling.

In DEM bonded-particle simulations, model dimensionality affects particle packing, contact networks, force transmission, crack development, and failure localization. While 2D models are computationally efficient, 3D models provide a more realistic representation of stress redistribution and fracture development, although at a higher computational cost. Therefore, comparing 2D and 3D BPM responses under a consistent calibration framework is important for evaluating the balance between computational efficiency and physical realism. Although DEM-based bonded-particle models are widely used to simulate rock behavior, most existing studies focus either on a single model dimensionality or on comparing different contact models under specific conditions. Direct and systematic comparisons between 2D and 3D bonded-particle models-particularly under a consistent calibration framework-remain limited. The main objective of this study is to investigate the model dimensionality on the behavior of bonded-particle models by comparing separately calibrated 2D and 3D simulations under identical uniaxial conditions. The comparison focuses on stress-strain response, strength characteristics, and fracture evolution, with the aim of identifying the differences and limitations associated with each modeling approach. This study aims to determine whether 2D models can accurately depict 3D rock behavior or whether substantial differences arise from inherent geometric and mechanical limitations, using a consistent calibration basis and evaluation framework.

2 Materials and Methods

2.1 Model Setup, Calibration, and Material Properties

Numerical simulations were carried out using the Particle Flow Code, PFC 7.0. Both 2D and 3D bonded-particle models were developed within the same PFC environment to allow a consistent comparison of model dimensionality. Laboratory data from siltstone samples of the Trakya Formation in Istanbul, Türkiye, were used to calibrate the model. The laboratory dataset was derived from laboratory tests on Cebeciköy siltstone and included eight representative uniaxial compression tests and eight Brazilian indirect tensile strength tests. Average laboratory values obtained from this dataset were used as the macroscopic target properties for numerical calibration. During the calibration procedure, a large number of iterative numerical trial simulations were performed by systematically adjusting the micromechanical parameters until the laboratory-derived macroscopic response was reproduced. After this iterative calibration stage, one final 2D UCS simulation and one final 3D UCS simulation were selected for the comparative assessment presented in this study.The material represents a fine-grained, low-porosity sedimentary rock commonly encountered in underground engineering projects in the region.

The tested siltstone has a dry unit weight of approximately 26.70 kN/m³, an effective porosity of 2.43%, and a P-wave velocity of 2.89 km/s. Uniaxial compression tests yielded an average peak strength of about 38 MPa at an axial strain of approximately 0.35%, with a Young's modulus of 11.3 GPa and a Poisson's ratio of 0.05. These properties were adopted as the target macroscopic parameters for calibration.Both two-dimensional (2D) and three-dimensional (3D) bonded-particle models were generated using comparable specimen geometries and particle size distributions to ensure consistency between simulations. In the 2D models, the material was represented by bonded circular particles, whereas spherical particles were used in the 3D models. The particle size range and model resolution were selected to balance computational efficiency and mechanical representativeness. Calibration was performed through an iterative trial-and-error procedure, in which micro-mechanical parameters such as contact stiffness, bond strength, and frictional properties were systematically adjusted to reproduce the target macroscopic response. The calibration was guided by previously reported BPM/PFC calibration approaches, while the final parameter set was refined based on the laboratory response of the selected siltstone (Ündül & Zengin, 2025, 2026; Zengin, 2022; Zengin & Erguler, 2017, 2022). The calibration focused on matching the elastic modulus, peak strength, and overall stress–strain behavior under uniaxial loading conditions. Particular attention was given to ensuring that both 2D and 3D models were calibrated using the same target properties and a consistent calibration, allowing a direct comparison of their mechanical responses.Following calibration, numerical simulations were conducted under strain-controlled loading conditions until peak strength and post-peak behavior were reached.

The UCS simulations were conducted using rigid loading walls representing the upper and lower platens. Axial compression was applied symmetrically by moving both the upper and lower rigid walls toward the specimen at a constant velocity of 0.05 m/s. The wall–particle friction coefficient was set to 0.4. Because rigid walls were used, platen deformation was not considered, and no additional end-restraint condition was imposed other than the wall–particle friction defined above. A damping coefficient of 0.7 was used to reduce dynamic effects during loading. The timestep was automatically determined using the PFC stable timestep criterion. To determine an appropriate loading rate, preliminary simulations were conducted at different wall velocities. The resulting stress–strain responses and the system's energy balance were evaluated, and a wall velocity of 0.05 m/s was selected because it provided a stable stress–strain response while maintaining quasi-static loading conditions. The simulations were continued beyond peak strength and terminated when the post-peak axial stress decreased to approximately 80% of the peak strength.

The model responses were evaluated with respect to stress–strain behavior, crack development, and failure patterns to assess the influence of model dimensionality. The calibration results, including comparisons between experimental and numerical stress–strain responses and the corresponding failure patterns, are presented in Figures 1 and 2, while the associated macroscopic and micromechanical parameters are summarized in Tables 1 and 2.

3 Results and Discussion

The calibrated 2D and 3D bonded-particle models reproduce the overall mechanical response of the siltstone under uniaxial compression with good agreement (Figure 1). Both models capture the linear elastic regime, peak strength, and post-peak softening trend. The 2D model slightly overestimates the peak strength (38.95 MPa), whereas the 3D model shows a minor underestimation (36.01 MPa) compared to the laboratory value of 37.83 MPa (Table 1). A similar trend is observed for the elastic modulus: the 2D model (11.52 GPa) closely matches the experimental value (11.3 GPa), while the 3D model (10.78 GPa) is slightly lower. The axial strain at peak stress is accurately reproduced in both cases (0.36% for 2D and 0.35% for 3D versus 0.35% experimentally), indicating that the calibration procedure effectively captures the macroscopic stress–strain behavior when the 2D and 3D models are calibrated against the same laboratory-derived target properties using a consistent calibration. The final micromechanical parameters obtained for the calibrated 2D and 3D models are summarized in Table 2.

Although there is good agreement at the macro scale, both models show significant differences in tensile behavior and damage initiation. The tensile strength is significantly overestimated, with values of 10.97 MPa for 2D and 10.10 MPa for 3D compared to the experimental value of 3.78 MPa (Table 1), resulting in tensile-to-compressive strength ratios of approximately 28%, whereas the laboratory ratio is about 10%. This overestimation is consistent with previous bonded-particle model studies, which reported that the classical parallel-bond formulation may produce unrealistically high tensile resistance and lower UCS-to-tensile strength ratios than those commonly observed in intact rocks (Cho et al., 2007; Potyondy & Cundall, 2004). This behavior is mainly related to the mathematical nature of the selected parallel-bond model, in which bond breakage and tensile resistance are governed by idealized contact-scale strength parameters. As a result, when the model is primarily calibrated to reproduce the compressive stress–strain response, the predicted tensile strength may remain higher than the laboratory-derived value. In addition, the absence of explicitly introduced initial flaws, weak planes, microcracks, or spatially variable bond properties may delay stress localization and contribute to overestimating tensile strength. Similarly, crack initiation stress is delayed in the numerical models, occurring at 21.56 MPa (~55% of UCS) in 2D and 18.49 MPa (~51% of UCS) in 3D, compared to approximately 11 MPa (~29% of UCS) experimentally. Similar shifts in crack initiation have been reported in DEM-based studies, where the onset of microcracking tends to occur at higher stress levels due to the simplified representation of bond breakage, contact interactions, and, possibly, microscale deficiencies in the sample (Jing & Hudson, 2002; Lisjak & Grasselli, 2014). These differences are consistent with the known limitations of the classical parallel-bond formulation, in which the bond structure calibrated for compressive response often leads to unrealistically high tensile resistance and delayed microcrack formation.

The more distributed failure pattern observed in the 3D model can be partially attributed to the larger particle assembly (~20,000 particles) compared to the 2D model (~5,000 particles), which increases the complexity of the contact network and promotes more distributed stress transfer. However, the primary reason lies in the system's inherent dimensionality. The 3D model provides additional degrees of freedom and a more complex force-chain structure, enabling stress redistribution in multiple directions, whereas the 2D model imposes a more constrained, planar localization of deformation. Further insight into the underlying failure mechanisms is provided by the combined visualization of fragmentation, tensile crack distribution, and contact-force magnitude (Figure 3).

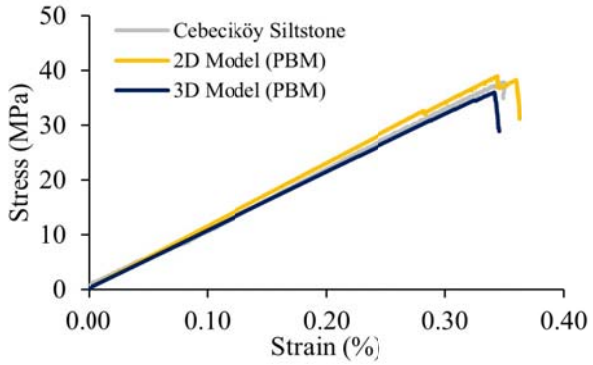


Fig. 1 Comparison of experimental and numerical stress–strain curves used for model calibration.

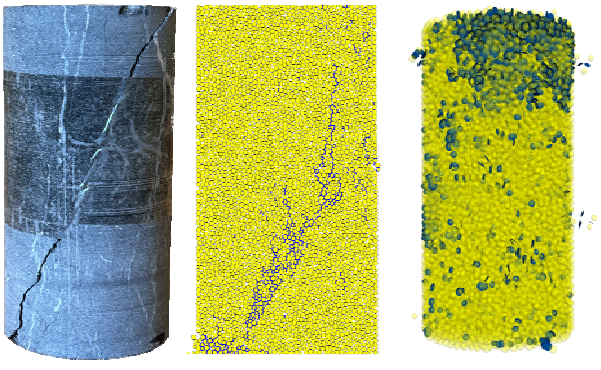


Fig. 2 Comparison of experimental and numerical failure patterns of samples (2D: 4498 balls, 3D: 19129 balls).

Table 1. Experimental target properties and corresponding macroscopic responses of the calibrated 2D and 3D bonded-particle models under uniaxial compression.

Parameter	**Laboratory**	**2D PBM**	**3D PBM**
Peak strength (MPa)	37.8	38.9	36.1
Young's Modulus (GPa)	11.3	11.5	10.8
Tensile strength (MPa)	3.8	10.9	10.1
Crack initiation stress (MPa)	11.0	21.6	18.49
Peak axial strain (%)	0.35	0.36	0.35

Table 2 Micro-mechanical parameters used in the bonded-particle models.

Parameter	**2D PBM**	**3D PBM**
Minimum and maximum particle size (m)	$0.8 - 1.6 \times 10^{-3}$	$2.0 - 3.0 \times 10^{-3}$
Radius multiplier (-)	1.0	1.0
Bond effective modulus (Pa)	8.3×10^{9}	1.1×10^{10}
Bond normal-to-shear stiffness ratio (-)	1.5	1.5
Bond tensile strength (Pa)	3.0×10^{7}	2.3×10^{7}
Bond cohesion-to-tensile strength ratio (-)	10	10
Friction coefficient (-)	0.4	0.4

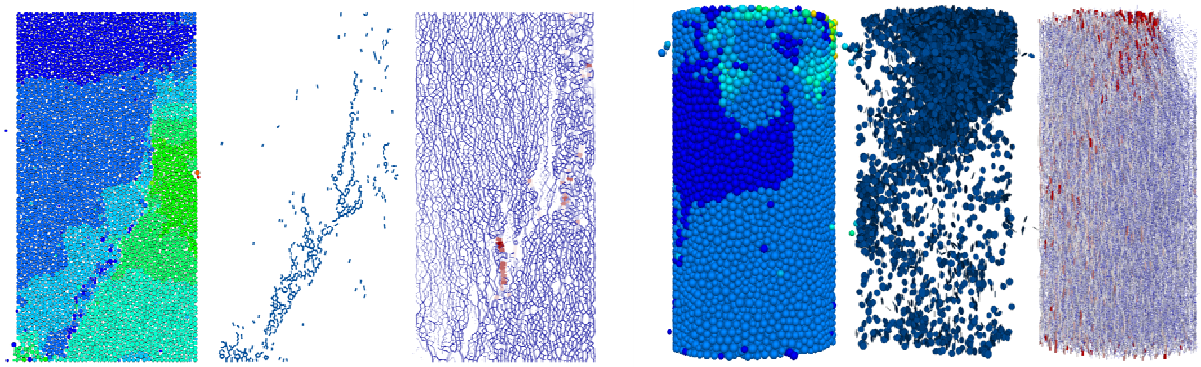


Fig. 3 From left to right: fragmentation, crack distribution, and contact-force magnitude for the 2D model, followed by the corresponding results for the 3D model at the final loading stage.

4 Conclusions

In both models, fragmentation develops in association with zones of intense crack activity, while the tensile crack networks define the primary paths of damage localization. Despite the compressive loading conditions, fracture development is dominated by tensile bond breakages, indicating that crack initiation and propagation are primarily controlled by local tensile stresses at particle contacts. This behavior is widely reported in both experimental and DEM-based rock simulations, where macroscopic shear failure emerges from the coalescence of tensile microcracks (Ündül & Zengin, 2025, 2026; Zengin & Erguler, 2022). Regions of elevated contact-force magnitude also coincide with areas of high crack density, highlighting the role of force-chain reorganization in driving damage evolution. This difference is also consistent with previous studies indicating that 3D DEM models support more complex force-chain structures and multidirectional stress redistribution, resulting in more diffuse damage patterns than in 2D simulations (Jing, 2003). Overall, both 2D and 3D bonded-particle models reproduced the global mechanical response of the siltstone with reasonable accuracy when calibrated against the same macroscopic laboratory targets. However, the final micromechanical parameter sets were not identical, reflecting the inherent differences between 2D and 3D particle assemblies in terms of packing, contact topology, coordination number, and force-chain development. Despite the comparable macroscopic response, important differences were observed in tensile behavior, crack initiation, and spatial damage localization. The 2D model produced a stronger and more continuous localization band, whereas the 3D model provided a more realistic representation of distributed fracture processes. These findings indicate that 2D models can be effective for capturing global mechanical behavior, while 3D models are better suited to representing complex fracture mechanisms. Laboratory observations consistently highlight the significant role of micro-texturally controlled variations in rock geomechanical properties (Ündül et al., 2013). Consequently, as widely emphasized in the literature, explicitly incorporating these micro-properties into numerical simulations is highly recommended for future research.

References

Cho, N., Martin, C. D., & Sego, D. C. (2007). A clumped particle model for rock. *International Journal of Rock Mechanics and Mining Sciences*, *44*(7), 997–1010. https://doi.org/10.1016/J.IJRMMS.2007.02.002

Cundall, P. A. &Strack, O. D. L. (1979). A discrete numerical model for granular assemblies. *Geotechnique*, *1*, 47–65.

Jing, L. (2003). A review of techniques, advances and outstanding issues in numerical modelling for rock mechanics and rock engineering. *International Journal of Rock Mechanics and Mining Sciences*, *40*(3), 283–353. https://doi.org/10.1016/S1365-1609(03)00013-3

Jing, L., & Hudson, J. A. (2002). Numerical methods in rock mechanics. *International Journal of Rock Mechanics and Mining Sciences*, *39*(4), 409–427. https://doi.org/10.1016/S1365-1609(02)00065-5

Kong, L., Shang, J., Ranjith, P. G., Li, B. Q., Song, Y., Cai, W., & Ling, F. (2024). Grain-based DEM modelling of mechanical and coupled hydro-mechanical behaviour of crystalline rocks. *Engineering Geology*, *339*, 107649. https://doi.org/10.1016/j.enggeo.2024.107649

Lisjak, A., &Grasselli, G. (2014). A review of discrete modeling techniques for fracturing processes in discontinuous rock masses. *Journal of Rock Mechanics and Geotechnical Engineering*, *6*(4), 301–314. https://doi.org/10.1016/J.JRMGE.2013.12.007

Potyondy, D. O. (2015). The bonded-particle model as a tool for rock mechanics research and application: current trends and future directions. *Geosystem Engineering*, *18*(1), 1–28. https://doi.org/10.1080/12269328.2014.998346

Potyondy, D. O., & Cundall, P. A. (2004). A bonded-particle model for rock. *International Journal of Rock Mechanics and Mining Sciences*, *41*(8 SPEC.ISS.), 1329–1364. https://doi.org/10.1016/j.ijrmms.2004.09.011

Qu, T., Feng, Y. T., Wang, M., & Jiang, S. (2020). Calibration of parallel bond parameters in bonded particle models via physics-informed adaptive moment optimisation. *Powder Technology*, *366*, 527–536. https://doi.org/10.1016/J.POWTEC.2020.02.077

Ündül, Ö., Amann, F., Aysal, N., &Plötze, M. (2013). Micro-textural controlled variations of the geomechanical properties of andesites. In *Rock Mechanics for Resources, Energy and Environment* (pp. 357–361). CRC Press. https://doi.org/10.1201/b15683-60

Ündül, Ö., & Zengin, E. (2025). The Influence of Strain Rate Variations on Bonded-Particle Models in PFC. *Geotechnics*, *4*(5). https://doi.org/10.3390/geotechnics5040082

Ündül, Ö., & Zengin, E. (2026). Bonded-particle modeling of sedimentary rocks: insights into model selection and mechanical response. *Mediterranean Geoscience Reviews 2026 8:1*, *8*(1), 35–54. https://doi.org/10.1007/S42990-025-00214-1

Vallejos, J. A., Salinas, J. M., Delonca, A., & Mas Ivars, D. (2017). Calibration and Verification of Two Bonded-Particle Models for Simulation of Intact Rock Behavior. *International Journal of Geomechanics*, *17*(4), 06016030. https://doi.org/10.1061/(asce)gm.1943-5622.0000773

Zengin, E. (2022). Usability Assessment of Different Contact Models for Modelling the Failure Behaviour of Sedimentary Rocks Under Unconfined Stress Conditions. *Yerbilimleri*, *43*(1), 61–75. https://doi.org/10.17824/YERBILIMLERI.1030332

Zengin, E., & Erguler, Z. A. (2017). Comparison of Crack Initiation, Propagation and Coalescence Behavior of Concrete and Rock Materials. *European Geosciences Union 2017*, *19*. https://meetingorganizer.copernicus.org/EGU2017/EGU2017-12090-2.pdf

Zengin, E., &Erguler, Z. A. (2022). Experimental investigation of pore-fracture relationship on failure behaviour of porous rock materials. *Bulletin of Engineering Geology and the Environment*, *81*(9), 351. https://doi.org/10.1007/s10064-022-02857-y